GO/rGO as Reinforcing Nanofiller in Aramid Fiber/Epoxy Resin Composite Systems

Gemma Sanjuan Gomez[1,2], Manuel Lis[1,*], Jiahui Li[2], Paul Coldea[2], Cristian Lopez De Prada[2], Jorge Fernandez[2], and Guido Ruffini[2]

[1]*Chemical Engineering Department, ESEIAAT, UPC*

[2]*The Forest Next S.L.*

Abstract: Compatibility between matrix and reinforcement plays an important role in final properties of composite materials, which is why many works are focused in modify- ing interfacial interactions between both components to achieve greater mechanical properties. In the present study, 0.3 wt% of GO/rGO particles are introduced in epoxy resin/aramid fiber composites to evaluate the capacity of GO/rGO as reinforcing fillers. XPS, SEM, TGA, tensile and flexural tests are utilized to characterize GO/rGO, aramid fiber, three epoxy resin matrix systems and all composites obtained. Enhancements of mechanical properties up to 80 % were achieved by combining digly- cidyl ether bisfenol A (DGEBA) + diglycidyl aniline (DGA) + m-xylendiamine matrix, aramid fiber reinforcement and GO/rGO.

Keywords : Polyaramid composites, Epoxy, GO, Molecular interactions, TGA/DTG.

INTRODUCTION

Enhancement of mechanical and physical properties of composite materials (CCMM) gained an important role in technological developments of the last decade [1]. Although CCMM have higher strength and stiffness compared to the most of other materials employed for the same proposes, they suffer from low damage tolerance, a low impact resistance and an almost null elasticity. Despite the issues mentioned, CCMM have been introduced in several industrial fields like construction and aeronautics.

Aramid fibers (AF) are widely utilized as polymer based CCMM beside carbon and glass fibers because of their excellent thermal and oxidative stability, flame resistance and superior mechanical and dielectric behavior [2,3]. Moisture absorption and high elongation to failure are also two of many distinctive features that AF possess because of its chemical structure, which is shown in Figure **1**. Amide functional groups that link aromatic rings allow formation of hydrogen bonds, consequently, AF is capable to absorb humidity. Moreover, these intermolecular forces are responsible of the helix structure that permit a slight stretch of the fibers before their rupture. According to the orientations of hydroxyl and amide groups, two main types of AF can be distinguished: Meta-Aramid, commercially known as Nomex; and Para-Aramid, popularly named Kevlar. The orientation of substituted groups influences on chemical and mechanical properties of AF [4]. Liu *et al*. [5] studied the effect of ultrasound treatment of AF during the winding process on the interface of AF/epoxy resin composites and obtained an increase of 13 % in interlaminar shear strength (ILSS).

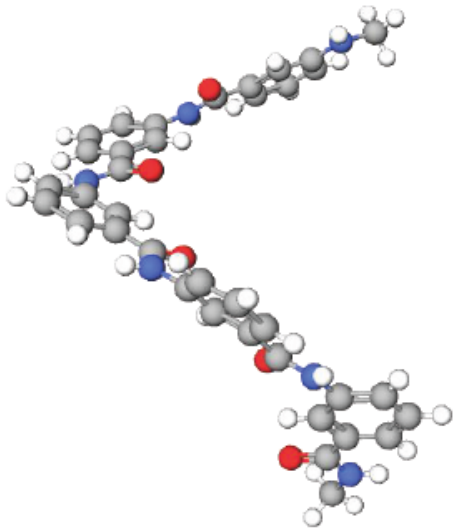

Figure 1: 3D Image AF.

Epoxy resins (ER) are thermoplastic polymers obtained from epichlorohydrin that have scarce industrial applications until their crosslinking reaction with a curing agent, also named as hardener (Hrd). The result of this reaction is a thermoset polymer highly employed in several fields. ER are usually phenol, amine and cycloaliphatic based, while Hrd can be Lewis acids/bases, amines or anhydrides [6]. Combinations of both compounds allow a wide variety of commercial ER.

*Address correspondence to this author at the Chemical Engineering Dept, ESEIAAT, Colon, 1, 08222 Terrassa;Tel: +34937398045;
E-mail: manuel-jose.lis@upc.edu

E-ISSN: 2309-3021/19

ER exhibit high synergy when interacting with AF, combining the best properties of both polymers. In pursuance of achieving higher mechanical and chemical properties of ER-AF composites or producing them for a lower cost without altering their performance, fillers are incorporated in CCMM systems.

Recent researches show that graphene is an excellent candidate to be used as reinforcing filler due to the improvement of CCMM properties [7] since it is considered as the strongest material ever known, with a tensile strength of 130 GPa [8]. However, graphene oxide (GO) and reduced graphene oxide (rGO) are considered as potential candidates to replace pris- tine graphene because of the similarity between them [9,10] and the plausibility of large-scale production at a lower cost. Additionally, due to the oxygen functional groups that their structures contain[11], higher dispersion grade of GO and rGO in the ER can be achieved.

Despite the variety of studies found about the effects of incorporating GO in CCMM [7,12–17], none of investigations found inquire into chemical and physical properties of AF composites modified with GO/rGO.

The aim of the present work is to analyze the effects generated by the addition of GO/rGO into three ER reinforced with AF by applying thermo gravimetric analysis (TGA), X-ray photoelectron spectroscopy (XPS), scanning electron microscopy (SEM) and tensile and flexural tests.

MATERIALS

In the present study, three matrix systems named X, Y and Z were selected, composition of each ER and Hrd is specified in Table **1**.

Table 1: Hardeners and Resins Compositions

ER/Hrd	Identification	Composition (%)
ER X	Diglycidyl ether bisfenol A	50 - 75
	Aniline diglycidyl ether	25 - 50
Hrd X	m-xylendiamine	25 - 50
	Bisphenol-A	10 - 25
	Benzyl alcohol	10 - 25
	Trimethylhexane-1,6-diamine	10 - 25
ER Y	Diglycidyl ether bisfenol A	50 - 90
	1,4-butanediol diglycidyl ether	10 - 25
Hrd Y	Polyethylenamine	25 - 50
	Polypropylene ether diamine	25 - 50
	3,6,9,12-tetraazatetradecane-1,14-diamine	10 - 25
ER Z	Diglycidyl ether bisfenol F	50 - 75
	Diglycidyl ether bisfenol A	25 - 50
Hrd Z	Polypropylene ether diamine	25 - 50
	Polyethylenamine	25 - 50

AF used as reinforcement of CCMM is a p-Aramid characterized by its twill style weave and surface weight of 300 g/cm^2.

Reinforcing fillers employed are 99 % pure flake-shaped GO/rGO nanopowder. Particle size distribution of GO/rGO is shown in the Figure **2**, GO particles are mainly distributed between 3 - 4 μm and a remarkable quantity of particles are of 1 μm while the number of particles with other sizes is considerably lower. Similar tendency is present in rGO size distribution, which has a high scope including sizes of 1 μm and between 2.5 - 4.5 μm.

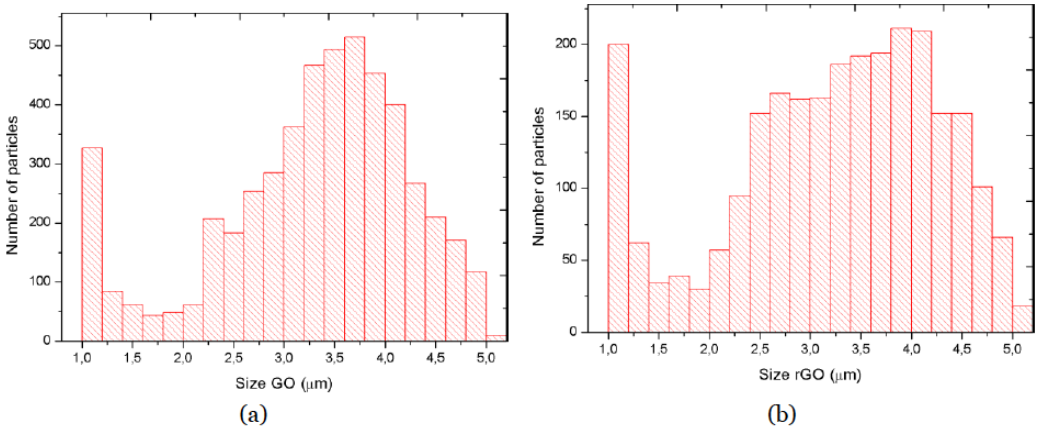

Figure 2: Size distribution of particles of the fillers: (**a**) GO particles; (**b**) rGO particles.

The XPS C1s scan applied involves the electron transition from carbon-oxygen atoms of different atomic configurations and its shape rely on their atomic densities. The deconvolu- tion of GO C1s spectra shown in figure Figure **3**(**a**) is splitting into 6 peaks, C=C double bond at 284.4 eV, C-C single bond at 284.8 eV, C-OH at 285.6, C-O-C at 286.7 eV, C=O double bond at 287.3 eV, and O-C=O at 288.6. rGO C1 spectra shown in Figure **3**(**b**) indicates that variety of chemical bonds in rGO is unaffected by the reduction process, but the quantity of oxidative bonds in rGO signal is lower in comparison with GO [17].

O1s scan was also applied to GO and rGO samples. The deconvolution of GO O1s spectra shown in Figure **3**(**c**) and Figure **3**(**d**), respectively. There are 2 peaks in both spectres: C=O double bond at 533.1 eV and C-OH at 531.2 eV. Signal strength is significantly lower in rGO in relation to GO, which confirms that the reduction process was carried out rightly.

Equipment

The Thermogravimetric Analysis was performed with TGA/SDTA851e Analyzer from Mettler Toledo, instrument run by STARe Software.

CY-500 Sonicator from Optic Ivienm System and T-10 basic ULTRA-TURRAX from IKA were employed to homogenize epoxy resin-GO/rGO systems.

Optical microscope model BX43 by Olympus and the software Advanced Image and Particles Size Analyzer (AIPSA) [18] were utilized to check the particle size of GO/rGO once dispersed into the matrix.

XPS experiments were performed in a PHI 5500 Multitechnique System (from Physical

Electronics) with a monochromatic X-ray source (Aluminium Kalfa line of 1486.6 eV energy and 350 W).

Scanning Electron Microscope model JSM-5610 by JEOL was employed to obtain high- resolution images of prepared samples surfaces.

Electro-mechanical materials testing machine fitted with a ball-screw drive from E se- ries by Zwick Roell Group was employed to determine the mechanical performance of the composites.

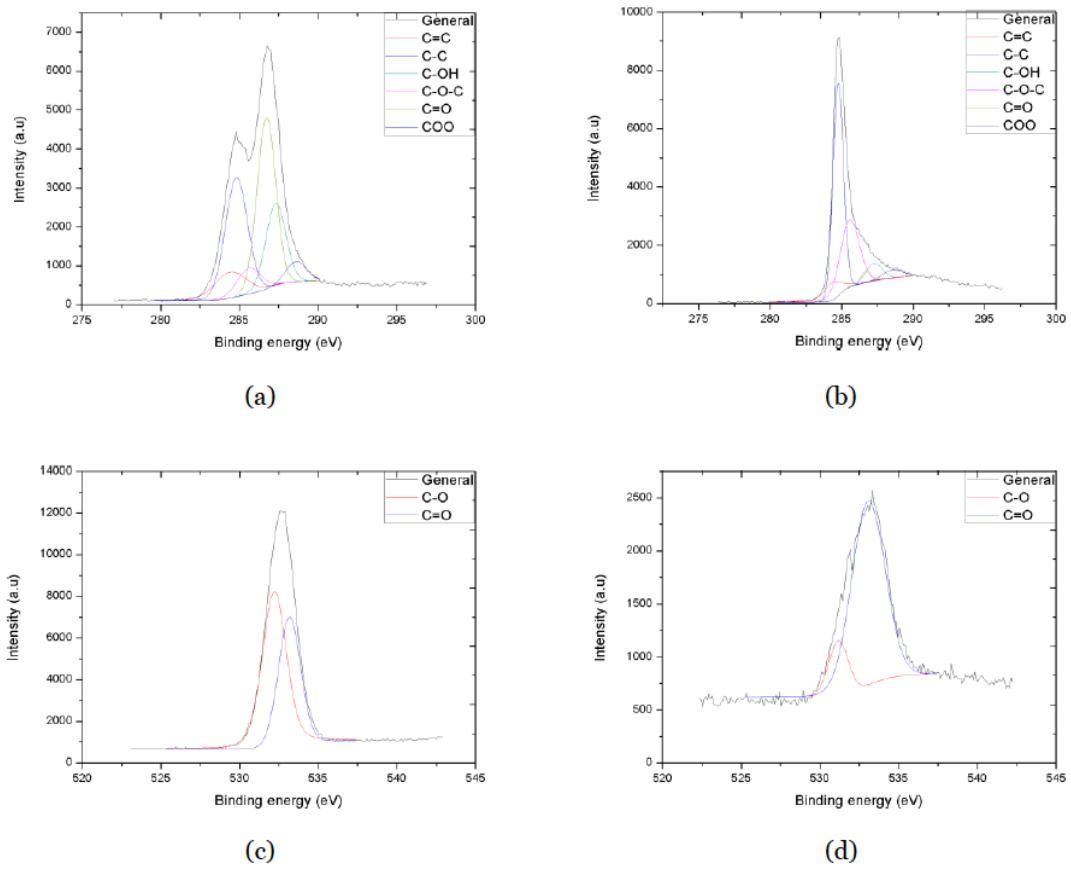

Figure 3: XPS characterization of fillers: (**a**) C1 of GO; (**b**) C1 of rGO; (**c**) O1 of GO; (**d**) O1 of rGO.

EXPERIMENTAL METHOD

Preparation of GO/rGO Modified AF/ER Composites

Dispersion of 0.3 wt% of GO/rGO in ER was the first step to elaborate modified CCMM; GO required 30 min of ultrasonication to achieve a homogeneous system, rGO needed an additional homogenizing process at speed of about 20500 rpm with Ultra Turrax to reach a microheterogeneous system. The following step was preparation of the matrix in consid- eration of the weight ratio indicated by the manufactured for each ER/Hrd mixture. Once that ER/Hrd and ER-GO/rGO-Hrd systems are ready, wet lay-up technique was applied to manually impregnate AF. Systems X and Y require 8 h at 80 °C after being laid during 24 h at room temperature to complete its cross linking reaction, whereas Z needs 16 h at 60 °C after the same precuring conditions. Preparation process is depicted schematically in the Figure **4**.

Determination of mechanical properties of the composites

Tensile and bending tests were performed on the obtained CCMM to determine changes in their mechanical properties.

Tensile tests were performed in accordance with specifications designated in ISO 527- 1:2012. Test specimens were taken from flat areas of composites, they had a width of 15 ±5 mm, an overall length of 250 mm and a thickness less or equal than 1 mm. The tests were conducted with a speed of 2 mm/min.

Three-point bending tests were conducted with a speed of 1 mm/min on specimens which dimensions were 100 × 15 × 2 mm, according to ISO 14125:1998.

XPS Analysis

GO and rGO were analyzed in a circle of 0.8 mm diameter. The selected resolutions for the spectra was 187.85 for Pass Energy and 0.8 eV/step for the general spectra and 23.5 eV for Pass Energy and 0.1 eV/step for the spectra of the different elements.

All Measurements were performed in an ultra-high vacuum (UHV) chamber pressure be- tween 5 × 10^{-9} and 2 × 10^{-8} Torr.

TGA Characterization

TGA was applied to characterize raw AF, ER/Hrd and elaborated CCMM. Samples about 10 mg were placed in aluminum oxide crucibles and then allocated on the microbalance of the analyzer. Thermal degradation experiments were performed from 25 to 1025 °C under air atmosphere at a heating rate of 20 °C/min [19,20]. SEM samples preparation SEM was used to analyze samples after the conduction of tensile tests. Specimens were taken from the fracture zone. Clean ruptures were vertically placed in the sample holder while transverse cracks were horizontally disposed. A thin film of gold was deposited by 30 min sputtering process onto the specimen before inserting the sample holder into the chamber of the microscope.

RESULTS AND DISCUSSION

Mechanical Properties

Young's Modulus, rupture stress and elongation to failure are information provided by the tensile test while flexural stress is obtained from the bending test;

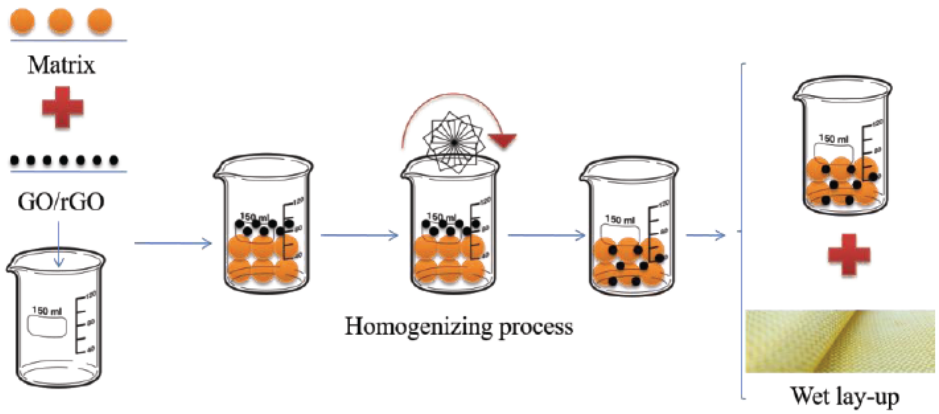

Figure 4: Preparation process scheme.

Table 2: Mechanical Properties of Non-Modified and GO/rGO Reinforced Composites

Composite	Youngs Modulus (GPa)	Rupture Stress (MPa)	Elongation to failure (%)	Bending Stress (GPa)
X-AF	13,4	214	1,7	8,4
X-GO-AF	24,6	317	2,3	14,7
X-rGO-AF	19,5	376	2,1	13,1
Y-AF	18,9	252	1,6	12,8
Y-GO-AF	19,2	397	2,1	15,5
Y-rGO-AF	21,5	384	1,9	12,0
Z-AF	20,6	377	1,9	13,6
Z-GO-AF	20,3	359	1,8	12,3
Z-rGO-AF	18,0	328	2,0	11,1

variations of mechanical properties due to the incorporation of GO/rGO were collected in the Table **2**.

First overview of mechanical results states that whereas GO/rGO influence positively in X and Y-AF, no remarkable variations can be appreciated in Z-AF. Going into details, all properties of X experienced a significant boost by the incorporation of GO, mechanical performance also improved by adding rGO, albeit a part from rupture stress that jumps from 214 to 376 MPa, which means rGO influences roughly 30 % more than GO in this particular case, general properties enhancement is minor. Furthermore, modified Y-AF exhibit a similar pattern without exceptions, since the slight variation in Young's Modulus is not meaningful. Observations mentioned above suggest that GO/rGO can be employed as reinforcing fillers to improve mechanical properties of CCMM indeed, but several factors determine their role in the system. The quantity of GO/rGO added depends on ER, higher percentage does not imply greater boosts, since mechanical performance of X-AF also betters with rGO, system X probably admits higher quantity of rGO than systems Y and Z before reaching saturation point [21], where rGO no longer acts as reinforcing filler. Other variables involved are undesired bonding of GO/rGO with a sizing agent of AF, and its dispersion and agglomeration grades [22].

Fracture surfaces of samples were obtained by SEM and shown in Figure **5**. Non-modified com- posites (Figure **5**(**a**)) break into two halves damaging all fibers of surrounding area, resulting in presence of micro-cracks that are perpendicular to the direction of applied load and multiple longitudinal splittings of filaments that constitute AF, which hints presence of interfacial cracks. Modified composites tear transversely leaving some undamaged fibers that preserve both parts together, micrograph in Figure **5**(**b**) shows that Z-rGO-AF also experiences fila- ments splitting. Furthermore,

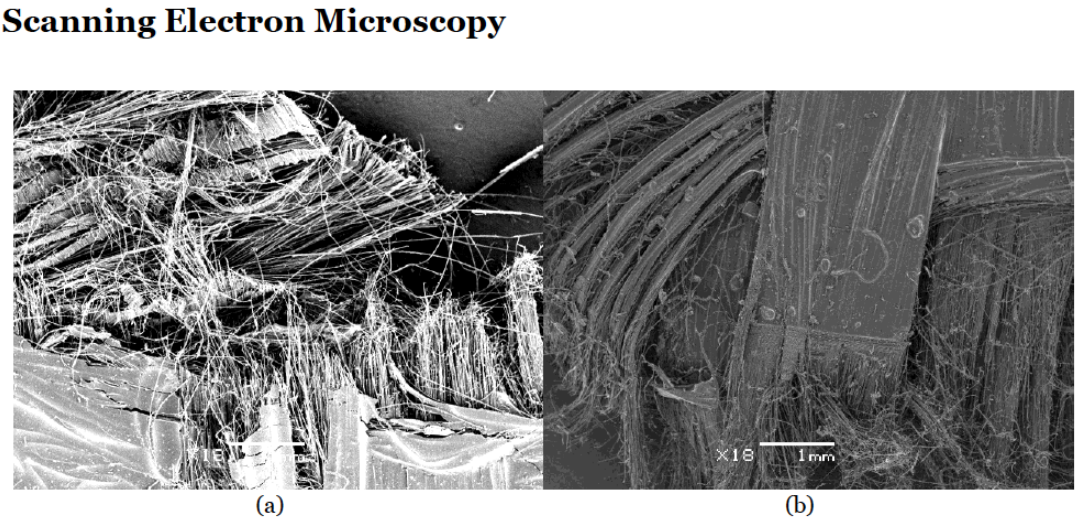

Figure 5: SEM images of fracture caused by applying tensile tests in: (**a**) Z-AF composite; (**b**) Z-rGO-AF composite.

several agglomerations of rGO particles can be appreciated in Figure **5**(**b**) while none is present in GO modified and non-modified samples.

A general overview of Figure **6** states that X-GO-AF present higher density of particles than Z-GO-AF and ER tends to form more and larger aggregations in all Z-AF CCMM. Moreover, the way that residual structure of matrix remains attached to micro-fibers after rupture varies from CM to CM; whereas residual ER envelopes micro-fibers partially as a continuous structure in modified CCMM, there is no evident attachment pattern in non- modified ones except from several aggregations of ER. Micrographs indicate that CCMM with higher density of well-dispersed particles exhibit better mechanical performance and the presence of

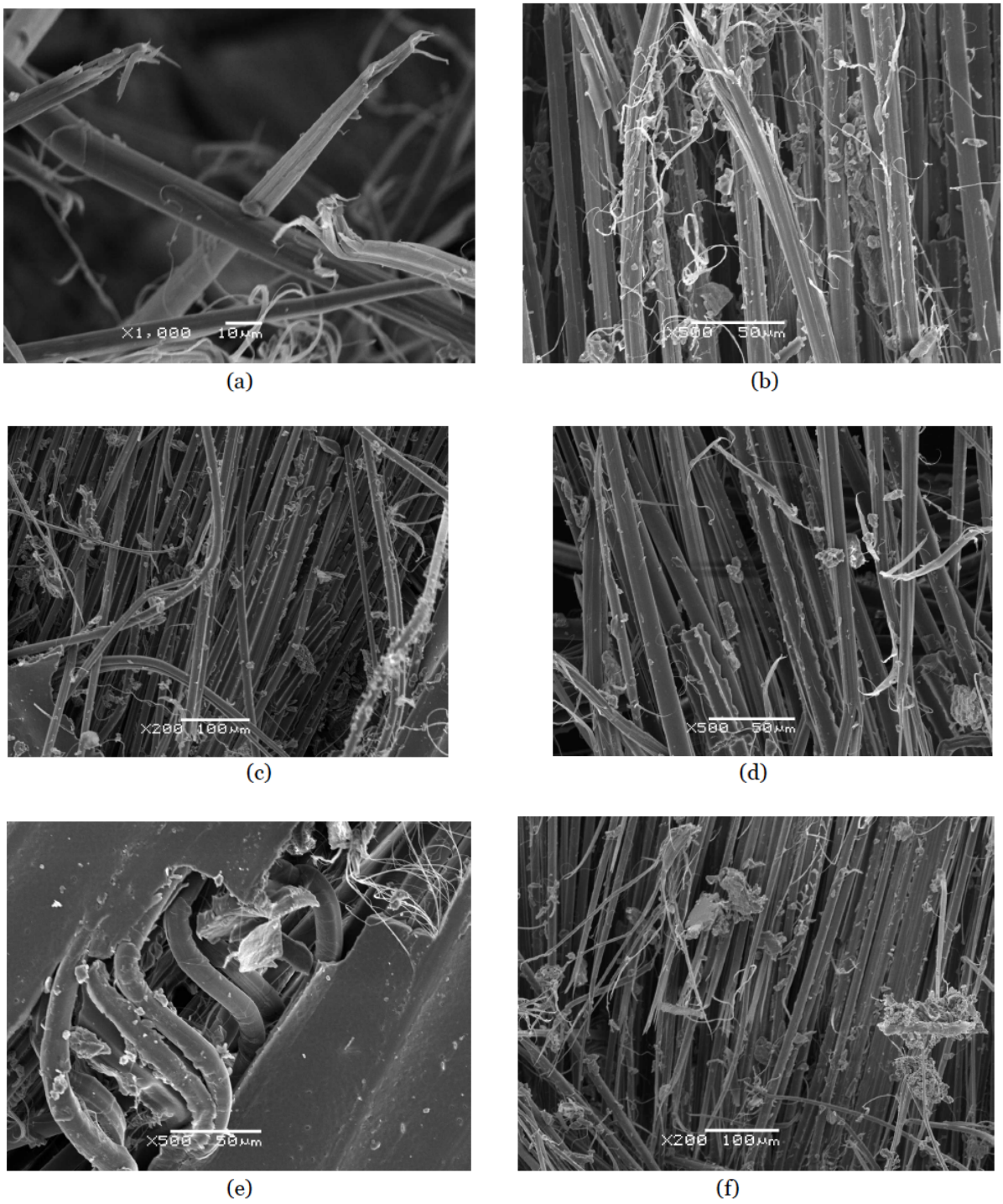

Figure 6: SEM images of composites obtained: (**a**) X-AF; (**b**) Z-AF; (**c**) X-GO-AF; (**d**) Z-GO-AF; (**e**) X-rGO-AF; (**f**) Z-rGO-AF.

Characterization of ER/Hrd systems

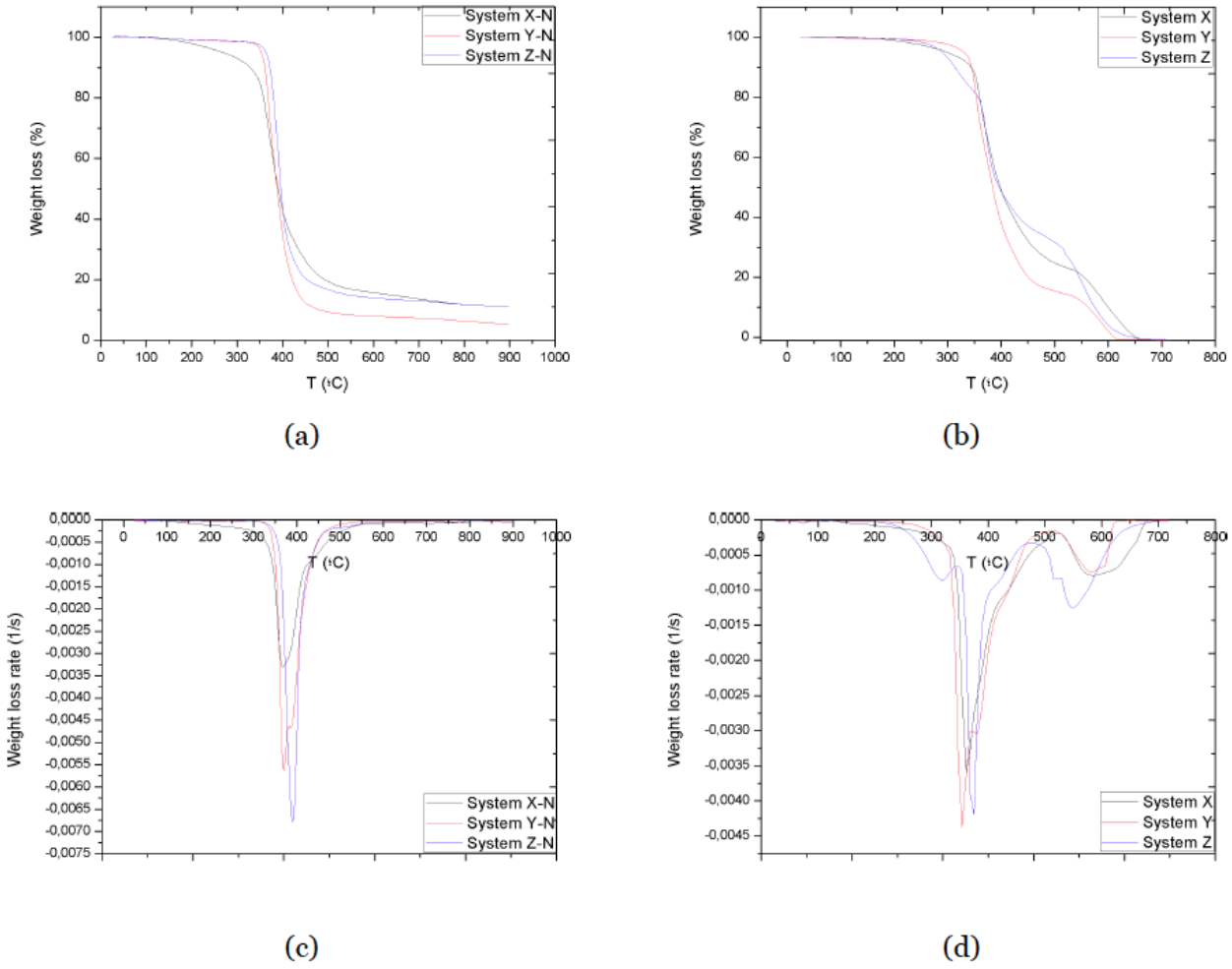

Figure 7: Thermogravimetric analysis of matrix systems: (**a**) and (**c**) under nitrogen atmo- sphere; (**b**) and (**d**) under air atmosphere.

aggregations cancels out the effect of GO/rGO as reinforcing fillers.

ER/Hrd systems were characterized by thermogravimetric analysis (TGA) from 25-900 °C with a heating rate of 20 °C/min under nitrogen atmosphere (Figure **7**(**a**)). First derivative of TGA (DTG) was applied to identify degradation regions more clearly, since each stage contains information about variety and quantity of interactions ruptured in a certain range of temperatures that TGA plot cannot provide. DTG shown in Figure **7**(**c**) states that all three ER/Hrd systems have one unique remarkable degradation phase at 370 °C for X and Y, and at 391 °C for Z. Furthermore, these regions are enclosed between approximately 350 and 500 °C, which hints that X, Y and Z contains similar variety of interactions, but the difference between their intensities states that, originally, Z had more interactions than Y, and both of them had more than X.

Oxidation behaviour of mentioned systems is also studied by performing the same ex- periment under air atmosphere (Figure **7**(**b**) and **7**(**d**)). Whereas X and Y present two main degradation stages, an additional low intensity phase can be identified in Z.

TGA and DTG plots of AF are shown in Figure **8**. Three degradation stages can be distinguished by reviewing DTG: the slight shoulder at approximately 520 °C corresponds to the cleavage of hydrogen bonds that hold polyaramid chains together; this low signal is attached to another one with a higher intensity at about 550 °C, assigned to the rupture of amide bonds that link aromatic rings of the backbone structure. Finally, a broad degradation stage at around 600 °C suggests the

Assessment of AF-based reinforcement

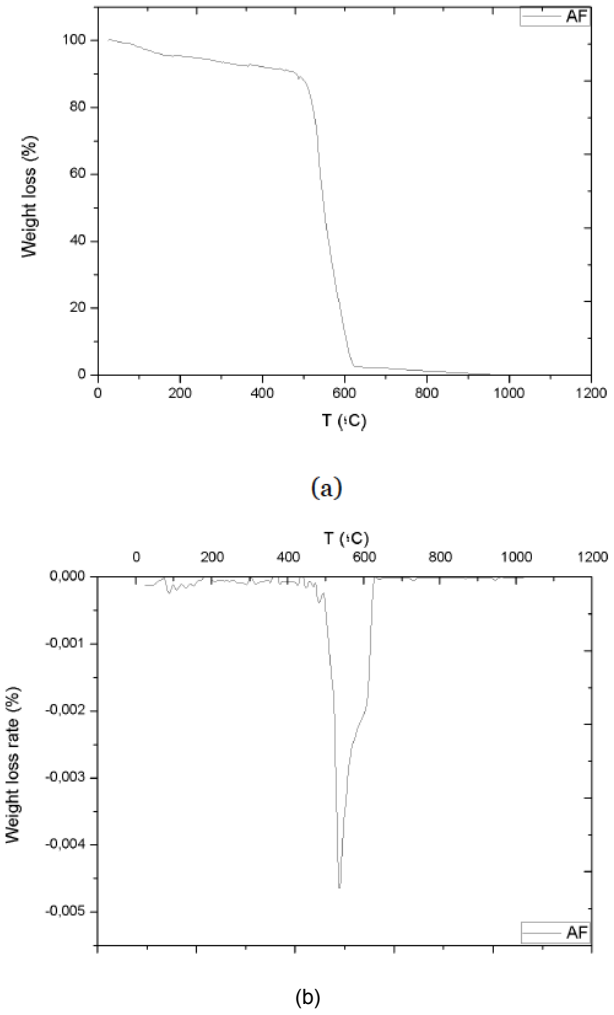

Figure 8: TGA of AF: (**a**) TGA curve; (**b**) DTG plot.

dehydrogenation of aromatic units to the complete decomposition of residual compounds [23].

DTG proved to reveal more detailed information about thermal behaviour of materials than TGA in previous sections, hence, in pursuance of finding out how GO/rGO influence in CCMM systems, the first derivative was utilized instead of TGA. Moreover, Advanced Analyzer of TGA (2ATGA) [24], a software that select and describe noticeable peaks with param- eters represented in Figure **10** was developed to accomplish a precise analysis of interactions involved in a degradation stage (W), quantity of chemical bonds decomposed (H) and the relation between them (A and MW). Table **3** shows data obtained about AF, ER/Hrd and non-modified CCMM, information regarding GO/rGO reinforced CCMM are collected in table Table **4**.

Analysis results reported by 2ATGA state that seven common degradation stages (partial areas) pertaining to cleavage of interactions or chemical bonds of the structure formed can be distinguished in all CCMM, independent of the matrix system applied:

- Partial Area 1, around 100 ˚C: the low intensity of this stage, the temperature where it takes place and the tendency of AF to absorb moisture suggest that it corresponds to the release of humidity present in the system [23].
- Partial Area 2, around 300 ˚C: the signal is rather weak, which indicates the presence of a few interactions between ER/Hrd and AF. The incorporation of GO/rGO modifies the stage slightly.

Characterization of CCMM

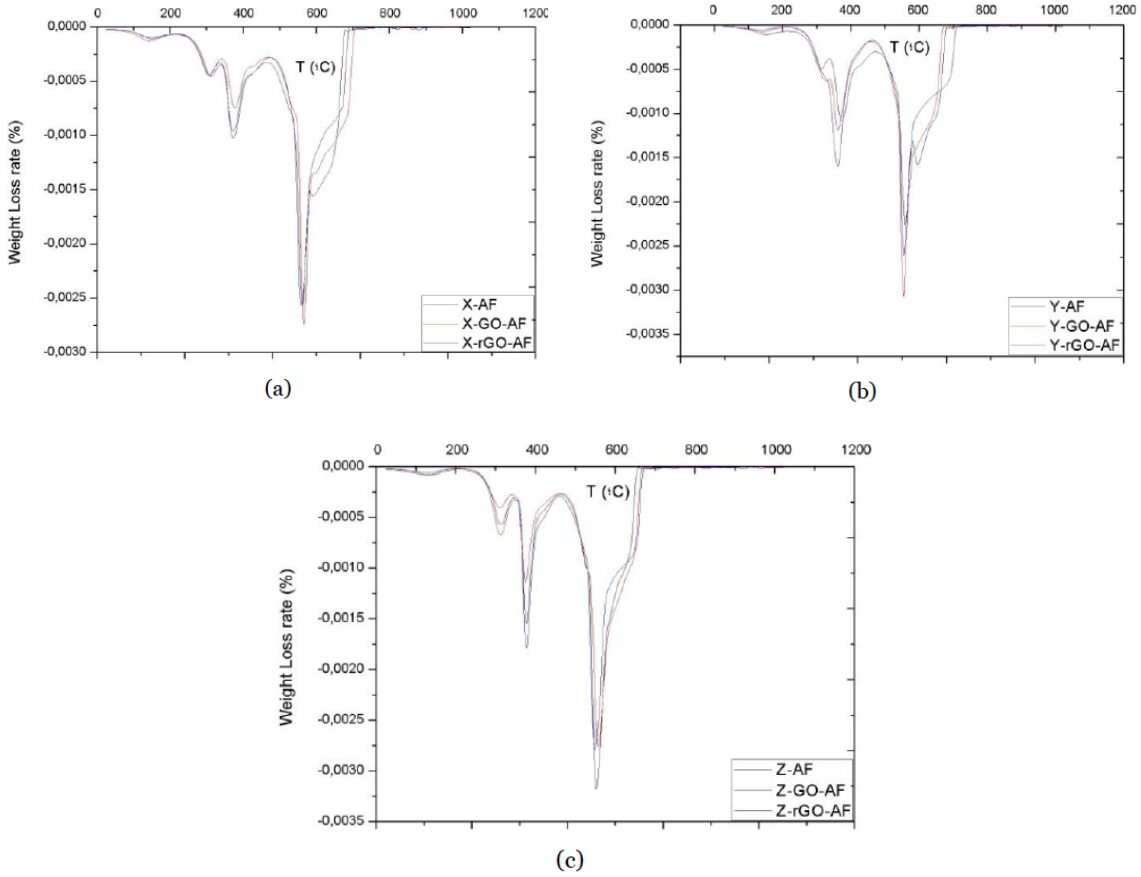

Figure 9: DTG of non-modified and reinforced composites: (**a**) X-AF and GO/rGO mod- ified X-AF composites; (**b**) Y-AF and GO/rGO modified Y-AF composites; (**c**) Z-AF and GO/rGO modified Z-AF composites.

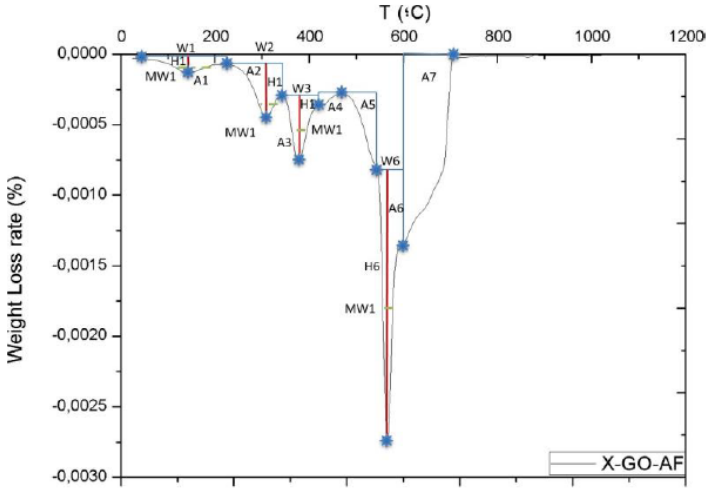

Figure 10: Representation of selected parameters in DTG of X-AF composite.

- Partial Area 3, around 380-400 °C: the high intensity of this stage hints cleavage of chemical bonds that pertain to ER/Hrd, since this signal also appears with a significant strength in DTG of cross-linked ER. The inclusion of GO/rGO has not influenced in this decomposition zone noticeably.

Table 3: DTG Data about AF, ER and non-Modified CCMM.*Although the Intensity of this Stage in the System is not as Significant as the other Ones, an Little Shoulder can be Appreciated

Composite	Partial Area Assignment	Temperature (°C)	H (1/s)	W (°C)	MW (°C)	A (°C/s)
AF	-	-	-	-	-	-
X	2	361	0.003588	476	315	-0.2565
	3	578	0.000599	161	63	-0.0831
X-AF	1	145	0.000091	170	100	-0.0004
	2	315	0.000390	120	100	-0.0115
	3	375	0.000668	140	40	-0.0273
	4*	-	-	-	-	-
	5*	-	-	-	-	-
	6	565	0.002249	110	90	-0.0756
	7	895	0.000022	190	10	-0.1127
Y	2	382	0.000033	147	14	-0.1651
	3	578	0.000589	112	70	-0.0511
Y-AF	1	145	0.000095	170	100	-0.0003
	2	315	0.000426	120	100	-0.0114
	3	375	0.000694	140	40	-0.0292
	4*	-	-	-	-	-
	5*	-	-	-	-	-
	6	555	0.001819	110	80	-0.0806
	7	595	0.000197	200	10	-0.1086
Z	1	319	0.000851	182	154	-0.0571
	2	375	0.003532	126	28	-0.1593
	3	550	0.000522	56	42	-0.0298
Z-AF	1	125	0.000062	130	80	-0.0087
	2	315	0.000265	120	30	-0.0304
	3	375	0.001253	210	90	-0.0708
	4*	-	-	-	-	-
	5*	-	-	-	-	-
	6	555	0.003137	50	120	-0.2209
	7*	-	-	-	-	-

- Partial Area 4, around 400-450 °C: the low intensity and the absence of this signal in AF suggest that it corresponds to the rupture of interactions between the residual structure of ER/Hrd and AF. This stage is barely affected by the presence of GO/rGO.

- Partial Areas 5, 6 and 7: these phases correspond to the thermal degradation process of AF. As described previously, intermolecular forces between polymer chains are rup- tured at first, then occurs the cleavage of amide functional groups and eventually, the degradation of aromatic rings happens [23].

Several patterns associate mechanical performance enhancements with modifications in DTG plots due to the presence of GO/rGO: a variation of about 11 % in the main area involves an increase in the properties; when no change occurs in the main area, a secondary area greater than half of a main one experiencing 11 % of variation is also linked to properties improvement; related

Table 4: DTG Data about GO/rGO modified CCMM.*Although the Intensity of this Stage in the System is not as Significant as the other Ones, an Little shoulder can be Appreciated

Composite	Partial Area Assignment	Temperature (°C)	H (1/s)	W (°C)	MW (°C)	A (°C/s)
X-GO-AF	1	145	0.000105	160	100	-0.0005
	2	305	0.000372	120	80	-0.0014
	3	375	0.000449	120	30	-0.0298
	4*	-	-	-	-	-
	5*	-	-	-	-	-
	6	565	0.002456	240	100	-0.0536
	7	715	0.000008	60	10	-0.2337
X-rGO-AF	1	145	0.000030	120	70	-0.0116
	2	305	0.000117	130	30	-0.0280
	3	375	0.000626	230	90	-0.0700
	4*	-	-	-	-	-
	5*	-	-	-	-	-
	6	555	0.002446	50	140	-0.2198
	7*	-	-	-	-	-
Y-GO-AF	1	135	0.000056	170	90	0.0003
	2	325	0.000603	120	110	-0.0076
	3	365	0.000547	130	30	-0.0288
	4*	-	-	-	-	-
	5*	-	-	-	-	-
	6	555	0.002905	210	90	-0.0727
	7*	-	-	-	-	-
Y-rGO-AF	1	135	0.000029	250	70	0.0062
	2*	-	-	-	-	-
	3	365	0.001384	260	90	-0.1113
	4*	-	-	-	-	-
	5*	-	-	-	-	-
	6	555	0.002609	60	160	-0.2102
	7*	-	-	-	-	-
Z-GO-AF	1	125	0.000067	150	70	-0.0085
	2	315	0.000341	110	30	-0.0356
	3	375	0.000874	270	80	-0.0565
	4*	-	-	-	-	-
	5*	-	-	-	-	-
	6	555	0.002706	40	170	-0.2297
	7*	-	-	-	-	-
Z-rGO-AF	1	315	0.000037	160	90	0.0005
	2	375	0.000382	140	110	-0.0063
	3	555	0.001474	110	30	-0.0259
	4*	-	-	-	-	-
	5*	-	-	-	-	-
	6	835	0.002359	220	90	-0.0774
	7*	-	-	-	-	-

to bending stress, modified CCMM are stiffer than non-modified ones if there is a decrease greater or equal to 10 % in the main area, otherwise, CCMM are more flexible.

CONCLUSION

Influence of the incorporation of GO/rGO in epoxy resin/aramid fiber composites was pon- dered in the present study and several conclusions can be extracted from experimental results obtained: the addition of GO/rGO particle not always involve enhancement of properties of the composite material, but when mechanical performance actually improves, a great boost in Young's modulus, rupture stress, elongation to failure and bending stress can be appreci- ated; the GO/rGO dispersion grade achieved is the main factor in properties enhancement, this in turn depends on geometry and size of particles; and TGA plots of composites indi- cate that the presence of GO/rGO modifies degradation temperatures of certain chemical structure, which hints existence of interactions between aramid fiber, GO/rGO and epoxy resin.

ACKNOWLEDGMENT

The authors are grateful to Ruffini S.L. for the financial support; to Zwick S.L. and Isidoro Soto for the permission to use their testing machine and publish the results; and to Torras Suministros Industriales S.L. for providing the material employed in the present study.

REFERENCES

[1] Mittal G, Dhand V, Rhee KY, Park S-J, Lee WR. A review on carbon nanotubes and graphene as fillers in reinforced polymer nanocomposites. J Ind Eng Chem. 2015; 21: 11-25. https://doi.org/10.1016/j.jiec.2014.03.022

[2] Khanna YP, Pearce EM, Smith JS. *et al*. Aromatic Polyamides. II. Thermal Degradation of some Aromatic Polyamides and their Model Diamides. J Polym Sci A Polym Chem. 1981; 19(11): 2817-34. https://doi.org/10.1002/pol.1981.170191115

[3] Yang HH. Aromatic High-strength Fibers. John Wiley & Sons, Inc., 1990,28(8): 264-5.

[4] S, P., KM, S., K, N., & S, S. Fiber Reinforced Composites - A Review. Journal of Material Science & Engineering, (2017): 06 (03)

[5] Liu L, Huang YD, Zhang ZQ, Jiang ZX, Wu LN. Ultrasonic treatment of aramid fiber surface and its effect on the interface of aramid/epoxy composites. Appl Surf Sci. 2008; 254(9): 2594-9. https://doi.org/10.1016/j.apsusc.2007.09.091

[6] Ellis B. New York: Springer 1993.

[7] Tang L-C, Wan Y-J, Yan D, Pei Y-B, Zhao L, Li Y-B, *al*. The effect of graphene dispersion on the mechanical properties of graphene/epoxy composites. Carbon. 2013; 60: 16-27. https://doi.org/10.1016/j.carbon.2013.03.050

[8] Lee C, Wei X, Kysar FW, Hone J. Measurement of the Elastic Properties and Intrinsic Strength of Monolayer Graphene. Science. 2008; 321(5887): 385-8. https://doi.org/10.1126/science.1157996

[9] Park S, Lee KS, Bozoklu G, Cai W, Nguyen AT, Ruoff RS. Graphene Oxide Papers Modified by Divalent Ions-Enhancing Mechanical Properties via Chemical Cross-Linking. ACS Nano. 2008; 2(3): 572-8. https://doi.org/10.1021/nn700349a

[10] Paci JT, Belytschko T, Schatz GC. Computational Studies of the Structure, Behavior upon Heating, and Mechanical Properties of Graphite Oxide. J Phys Chem C. 2007; 111(49): 18099-111. https://doi.org/10.1021/jp075799g

[11] Gao W. The Chemistry of Graphene Oxide. 2015. 61-95 p. https://doi.org/10.1007/978-3-319-15500-5

[12] Xu JY, Liu J, Li KD, Miao L, Tanemura S. Novel PEPA-functionalized graphene oxide for fire safety enhancement of polypropylene. Sci Technol Adv Mater. 2015; 16(2): 025006. https://doi.org/10.1088/1468-6996/16/2/025006

[13] Chen C-T, Martin-Martinez F, Ling S, Qin Z, J Buehler M. Nacre-inspired design of graphene oxide–polydopamine nanocomposites for enhanced mechanical properties and multi-functionalities. 2017; 1(1): 011003.

[14] Abdullah SI, Ansari MNM. Mechanical properties of graphene oxide (GO)/epoxy composites. HBRC Journal. 2015; 11(2): 151-6. https://doi.org/10.1016/j.hbrcj.2014.06.001

[15] Zhang X, Fan X, Yan C, Li H, Zhu Y, Li X, *et al*. Interfacial Microstructure and Properties of Carbon Fiber Composites Modified with Graphene Oxide. ACS Appl Mater Interfaces. 2012; 4(3): 1543-52. https://doi.org/10.1021/am201757v

[16] Ahmadi-Moghadam B, Sharafimasooleh M, Shadlou S, Taheri F. Effect of functionalization of graphene nanoplatelets on the mechanical response of graphene/epoxy composites. Mater Des (1980-2015). 2015; 66: 142-9. https://doi.org/10.1016/j.matdes.2014.10.047

[17] Monfared Zanjani JS, Okan BS, Menceloglu YZ, Yildiz M. Nano-engineered design and manufacturing of high-performance epoxy matrix composites with carbon fiber/selectively integrated graphene as multi-scale reinforcements. RSC Adv. 2016; 6(12): 9495-9506. https://doi.org/10.1039/C5RA23665G

[18] Sanjuan Gomez, G. Advanced image and particles size analyze. The Forest Next. (2018).

[19] Bekyarova E, Thostenson ET, Yu A, Itkis ME, Fakhrutdinov D, Chou T-W, *et al*. Functionalized Single-Walled Carbon Nanotubes for Carbon Fiber−Epoxy Composites. J Phys Chem C. 2007; 111(48): 17865-71 https://doi.org/10.1021/jp071329a

[20] Ogasawara T, Moon S-Y, Inoue Y, Shimamura Y. Mechanical properties of aligned multi-walled carbon nanotube/epoxy composites processed using a hot-melt prepreg method. Compos Sci Technol. 2011; 71(16): 1826-33. https://doi.org/10.1016/j.compscitech.2011.08.009

[21] Pathak AK, Borah M, Gupta A, Yokozeki T, Dhakate SR. Improved mechanical properties of carbon fiber/graphene oxide-epoxy hybrid composites. Compos Sci Technol. 2016; 135: 28-38. https://doi.org/10.1016/j.compscitech.2016.09.007

[22] Chen L, Chai S, Liu K, Ning N, Gao J, Liu Q, *al*. Enhanced Epoxy/Silica Composites Mechanical Properties by Introducing Graphene Oxide to the Interface. ACS Appl Mater Interfaces. 2012; 4(8): 4398-404. https://doi.org/10.1021/am3010576

[23] Villar-Rodil S, Paredes JI, Martínez-Alonso A, Tascón JMD. Atomic Force Microscopy and Infrared Spectroscopy Studies of the Thermal Degradation of Nomex Aramid Fibers. Chem Mater. 2001; 13(11): 4297-304. https://doi.org/10.1021/cm001219f

[24] Sanjuan Gomez, G. Analyzer of TGA. The Forest Next. (2018).

Received on 25-01-2019 Accepted on 04-03-2019 Published on 25-04-2019

DOI: https://doi.org/10.31437/2415-5489.2019.05.2